

## Dynamics of DNA replication loops reveal temporal control of lagging-strand synthesis

### Methods

**Protein expression and purification.** Previously published expression and purification protocols were used to prepare T7 DNA polymerase (1:1 complex of gp5 protein and *E. coli* trx)<sup>18</sup>, gp4<sup>19</sup>, and gp2.5<sup>20</sup>.

**Single-molecule stretching and length measurements.** Phage  $\lambda$  DNA molecules were annealed and ligated to modified oligonucleotides to introduce a biotinylated fork on one end of the DNA and a digoxigenin moiety on the other end as described previously<sup>5</sup>. The resulting DNA molecules were attached with the 5' terminus of the bifurcated end to the streptavidin-coated glass surface of a flow cell and with the 3' end of the same strand to a 2.8  $\mu\text{m}$  diameter anti-digoxigenin-coated paramagnetic bead (Dyna) (Figure S1a). To prevent nonspecific interactions between the beads and the surface, a 1 pN magnetic force on the bead was applied upward by positioning a permanent magnet above the flow cell. Beads were imaged with a CCD camera at a time resolution of 500 ms and their positions were determined by particle-tracking software (Semasopt). Coordinated DNA synthesis in the flow cell was carried out by flowing gp4 helicase/primase (10 nM hexamers), T7 DNA polymerase (a purified 1:1 complex of gp5 and thioredoxin) (80 nM), and gp2.5 (750 nM), in buffer A (40 mM Tris-HCl (pH 7.5), 10 mM  $\text{MgCl}_2$ , 10 mM DTT, 50 mM potassium glutamate (pH 7.5), 0.1 mg/ml BSA), 600  $\mu\text{M}$  each of dATP, dCTP, dGTP, dTTP) and 300  $\mu\text{M}$  of ATP and CTP. Traces were corrected for instabilities in the flow by subtracting traces corresponding to tethers that were not enzymatically altered. Brownian motion and residual fluctuations resulted in a 300 bp error in DNA length measurement.

**Fluorescence imaging.** DNA was tethered at the forked end to functionalized cover slips as described above, but beads were omitted. Instead, the hydrodynamic drag on the DNA itself was used to extend the molecule. In the presence of 100 nM Sytox Orange dsDNA-specific stain (Invitrogen), the stretched DNA was imaged using through-objective TIRF microscopy (Olympus IX-71; 60x 1.45 N.A.). A CW 532 nm diode laser (Crystalaser) was used to excite stain at power densities sufficiently low to minimize photo-induced cleavage of stained DNA over the time scale of an experiment. Protein and nucleotide concentrations were identical to those used to replicate the bead-tethered DNA molecules (see above). Single-molecule bead-tethering assays demonstrated that the kinetics of leading-strand synthesis and coordinated replication were not influenced by the presence of the stain (Supplementary Information).

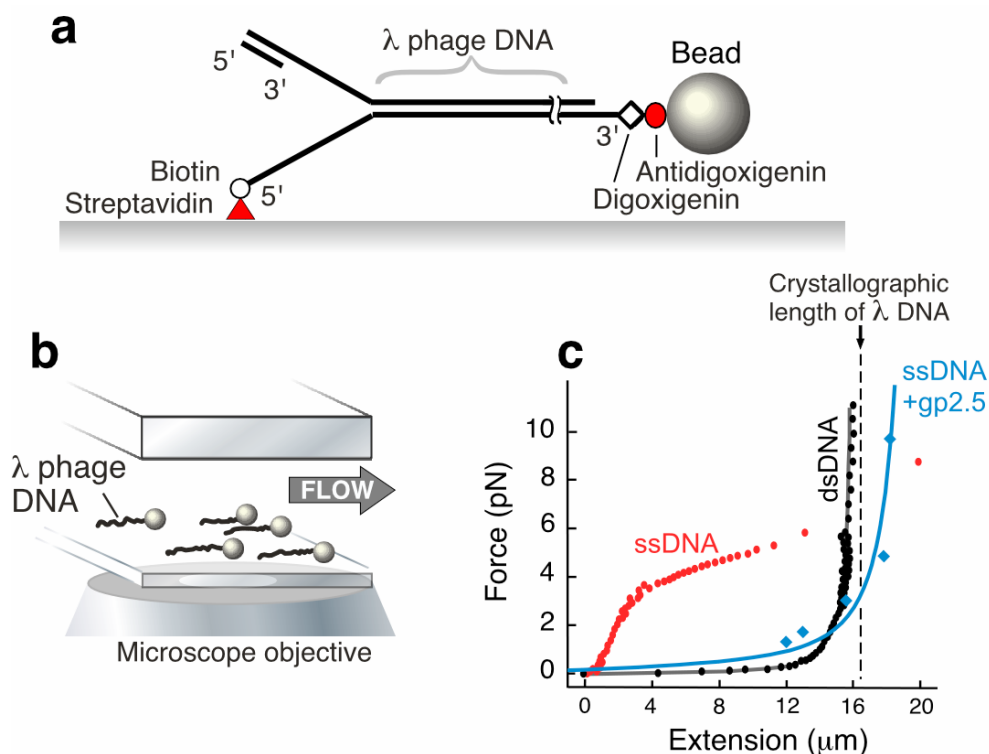


**Figure S1.** (a) Experimental design. Duplex  $\lambda$  phage DNA (48.5 kb) is modified to contain a replication fork with a primer to initiate leading-strand synthesis and a ssDNA segment to load the helicase on the lagging strand as described previously.<sup>1</sup> The lagging strand is attached to the surface via the 5' end of the fork using a biotin-streptavidin linker. The opposite end of the lagging strand is coupled to a paramagnetic bead using a digoxigenin-antidigoxigenin linker. (b) Schematic representation of the experimental arrangement (not drawn to scale). Tethered DNA molecules are stretched by applying a laminar flow of buffer over the surface. The length of individual DNA molecules is monitored by tracking the positions of the beads. A magnet is placed above the flow cell to exert a 1 pN force directed upwards, preventing the bead to nonspecifically interact with the surface. (c) Extension of  $\lambda$ -phage double-stranded DNA (dsDNA; black circles) and single-stranded DNA (ssDNA) without (filled red circles) and with (filled blue squares) gp2.5 ssDNA binding protein as a function of the total applied stretching force. The dashed vertical line at 16.2  $\mu\text{m}$  represents the crystallographic length of B-form  $\lambda$ -phage dsDNA. The small angle of the stretched DNA with respect to the surface is taken into account in the conversion from apparent to physical lengths. The single-stranded  $\lambda$  DNA template is generated by carrying out leading-strand synthesis on surface-tethered  $\lambda$  DNA containing a replication fork using gp4 helicase/primase and T7 DNA polymerase as described previously<sup>1</sup>. At the conclusion of strand-displacement synthesis, the flow cell was washed excessively with buffer to remove any residual protein. Gp2.5 was then flowed at 750 nM and length change of the ssDNA was measured at different stretching forces. At stretching forces between 1 and 3 pN, the length of gp2.5-coated ssDNA approaches that of dsDNA. At these stretching forces, conversion between ssDNA and dsDNA will not give rise to any appreciable length changes in the DNA, leaving loop formation as the only mechanism of length change. Fitting the force-dependent extension of gp2.5-coated ssDNA using the Worm-Like Chain model<sup>2</sup> (blue line for gp2.5-coated ssDNA, grey line for dsDNA) results in a persistence length of  $9 \pm 6$  nm, significantly shorter than that of dsDNA ( $\sim 50$  nm)<sup>2</sup> but higher than the 1-3 nm persistence length of ssDNA<sup>3,4</sup>.

## Observation of replication loops

### (a) Detection of loop formation

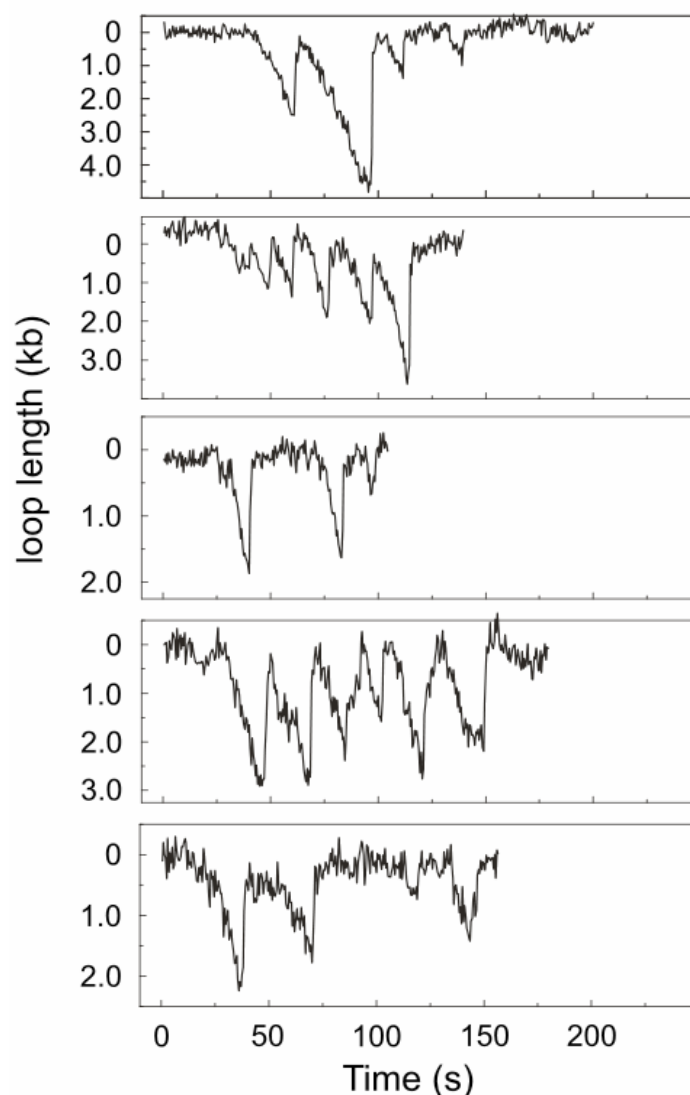


**Figure S2.** Five examples of time courses of the length of a single DNA molecule during leading- and lagging-strand synthesis. The DNA shortening corresponds to loop growth and is followed by a rapid length increase when a loop is released (schematically depicted in Figure 1a in the main text).

Brownian motion and residual flow instabilities resulted in an error in DNA length measurement of 300 bp (standard deviation). To ensure the incorporation of only bona fide loop-formation events into our data set, we only considered loops larger than 1 kb in our analysis. Assuming a normal distribution of the noise, this threshold results in a less than 1% probability of a false-positive detection of a loop. To exclude a bias in loop length analysis resulting from under sampling small loops, we also excluded loops with length less than 1 kb from the fitting of loop length distributions.

Our ability to observe loop formation relies on the absence of a difference in length between dsDNA and gp2.5-coated ssDNA. Even though the absolute length of dsDNA and gp2.5-coated ssDNA varies significantly over the forces used in our study, the length difference between the two forms of DNA remains less than 5% of the DNA length (Figure S1c). At 1.7 pN, the force at which all the kinetic

characterization was performed, the length difference between the typical amounts of ssDNA and dsDNA interconverted during coordinated replication becomes significantly less than the other experimental noise contributions. Moreover, this small difference in dsDNA/ssDNA lengths will be visible only in the very first replication loop in every trace: only prior to the formation of the first replication loop, net ssDNA template will be generated through leading-strand synthesis. From there on, leading-strand synthesis will always create as much new ssDNA as lagging-strand synthesis converts back to dsDNA, ensuring that there is no net change in the ratio of dsDNA/ssDNA.

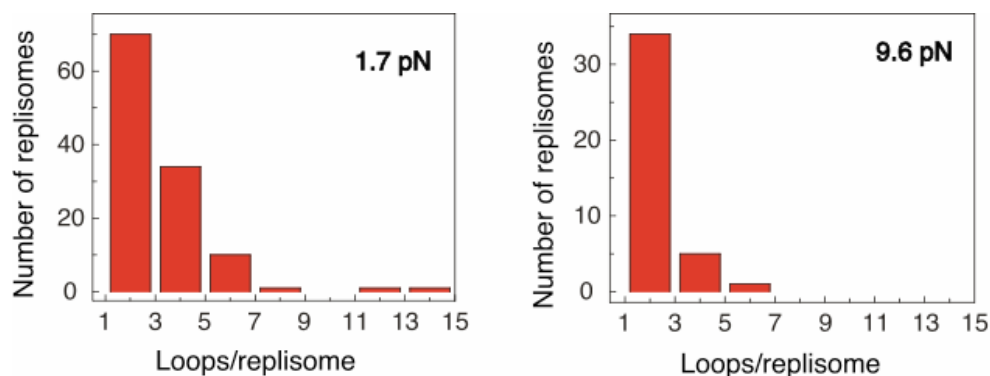
The rate of loop formation was measured to be 146 bp/s (see main text Figure 1e for rate distribution). The rate of leading-strand synthesis under the same conditions (i.e., with DNA polymerase in solution) has been measured by our group to be 80 bp/s (see Figure 4 in Ref. 1). It is important to note that this rate is significantly reduced compared to the leading-strand synthesis rate in the absence of any DNA polymerase in solution (164 bp/s; Ref 1, Figure 3). A possible explanation for this slowing down of leading-strand synthesis with increasing DNA polymerase concentration is that the association of free DNA polymerases with available binding sites on the hexameric gp4 reduce the helicase rate. The observation that the 80 bp/s leading-strand synthesis rate is close half of the 146 bp/s loop formation rate is consistent with leading-strand synthesis being responsible for half of the loop formation rate.

### **(b) Slow-down of loop release**

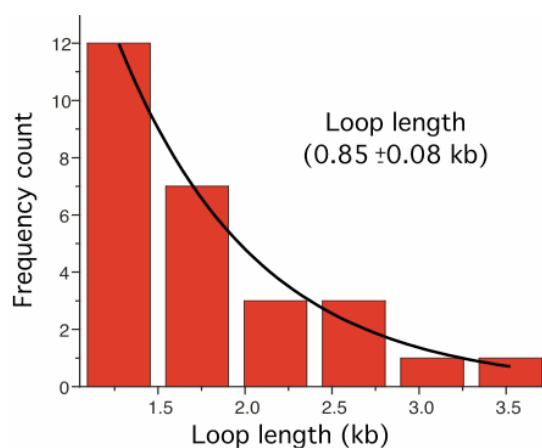
Occasionally, upon loop release we do not observe an instantaneous DNA lengthening, but rather a gradual return to the DNA's original length (for example, see trace in Figure 1b, main text). These 'slow' loop releases were rare (less than 5%) and may be caused by the formation of a compact 'superstructure' of gp2.5 at the replication fork, similar to those previously observed by EM.<sup>5</sup> Upon loop release, the gp2.5 structure needs to be destabilized first before the DNA can revert to its full length, a process that may take a few 100 ms. The duration of these slow loop releases are negligible in duration compared to the lag times between loop release and formation and thus do not impact our analysis of the replication-loop kinetics.

### **DNA shortening depends on primase and DNA polymerization activities**

- 1) The decrease in DNA length depends on DNA polymerase activity. Upon addition of the 2',3'-dideoxynucleotide chain terminator ddTTP<sup>7</sup> no DNA shortening was observed, indicating that the observed loop formation is dependent on DNA synthesis activity by T7 DNA polymerase. DNA unwinding by gp4 is not influenced by ddTTP,<sup>8</sup> demonstrating that the observed changes in DNA length are not caused by helicase activity alone.
- 2) DNA shortening depends on primase activity. In the absence of ribonucleotides, the frequency of occurrence of traces containing replication loops is reduced 10-fold with no single replisome containing more than one replication loop. The infrequent loop formation that occurs in the absence of primase activity could correspond to loops comprised exclusively of ssDNA that have been observed in EM studies in the T4 and T7 replication systems.<sup>5,6,9,10</sup>

**Dependence of replisome processivity on applied force**

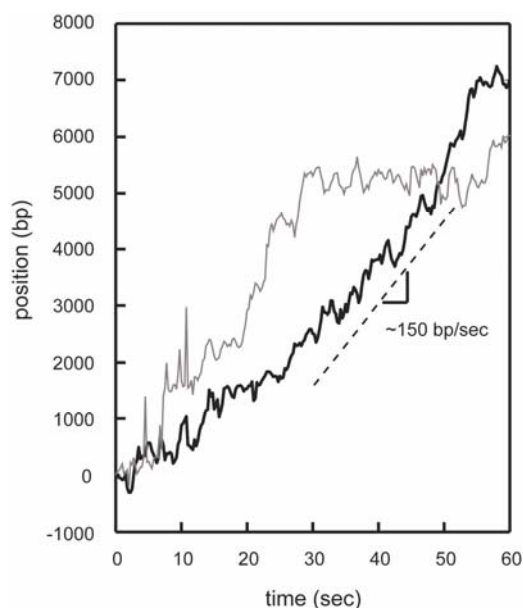
**Figure S3.** Replisome processivity, as defined as the number of loops formed per replisome. Histograms showing the number of loops per replisome obtained at forces of 1.7 pN ( $2.7 \pm 1.9$  loops/replisome with 25% of replisomes displaying more than 4 replication loops) and 9.6 pN ( $1.6 \pm 0.9$  loops/replisome with only 5% of replisomes displaying more than 4 replication loops). The 300-bp noise floor in our experiment makes it difficult to score loops with a length of a few hundred base pairs, resulting in an underestimation of the number of loops formed per replisome. The data suggests that the presence of a stretching force may inhibit loop initiation and reduce replisome processivity. Nevertheless, the processivity at a stretching force of 1.7 pN is of the same order of magnitude as the average of 6 Okazaki fragments per DNA molecule observed in T4 replication using electron microscopy (Chastain et al., *Mol Cell* 2000; v6, p803).

**Time-resolved fluorescent measurements of DNA synthesis****(a) Effect of staining the DNA with Sytox Orange on the length of replication loop**

**Figure S4.** In the main text (Fig. 2), we showed by staining the dsDNA with Sytox Orange stain (Invitrogen) that leading and lagging strand synthesis are taking place simultaneously. To ensure that the stain has no major effect on loop formation, we ensured that in the presence of the same amount of stain (100 nM) as in the fluorescence experiments, replication loops were still formed, indicative of bona fide coupled replication on both the leading and lagging strand. The average loop length was  $0.9 \pm 0.1$  kb, compared to  $1.4 \pm 0.1$  kb obtained in the absence of stain.

**(b) An example of a movie from the time-resolved fluorescence images of DNA synthesis**

Individual  $\lambda$  DNA molecules are fluorescently stained by means of intercalating dye, stretched by flow and imaged through Total Internal Reflection Fluorescence (TIRF) microscopy. The region of increased intensity corresponds to regions ahead of the fork where the flow stretches the leading-strand dsDNA product and aligns it with the parental dsDNA. The area of doubled intensity travels towards the end of the DNA, consistent with a processive replisome. Acquisition time per frame is 500 ms.

**(c) Examples of tracking the time-resolved fluorescence images of DNA synthesis**

**Figure S5.** Quantification of fork motion from fluorescence data. Projections of the DNA image (as shown in Fig. 2 in the main text) were fit by subtracting the  $t=0$  sec projection, leaving the intensity due to newly synthesized DNA. Gaussian fitting of this residual yielded the curve shown in this Figure. The rate of leading- and lagging-strand synthesis is calculated from fitting the slope and is consistent with that observed from the bead assay (Fig. 1c in the main text). Leading- and lagging-strand synthesis were observed in  $\sim 20\%$  of the surface tethered DNA in the presence of Sytox stain and laser illumination.

**Bulk-phase detection of coordinated DNA synthesis**

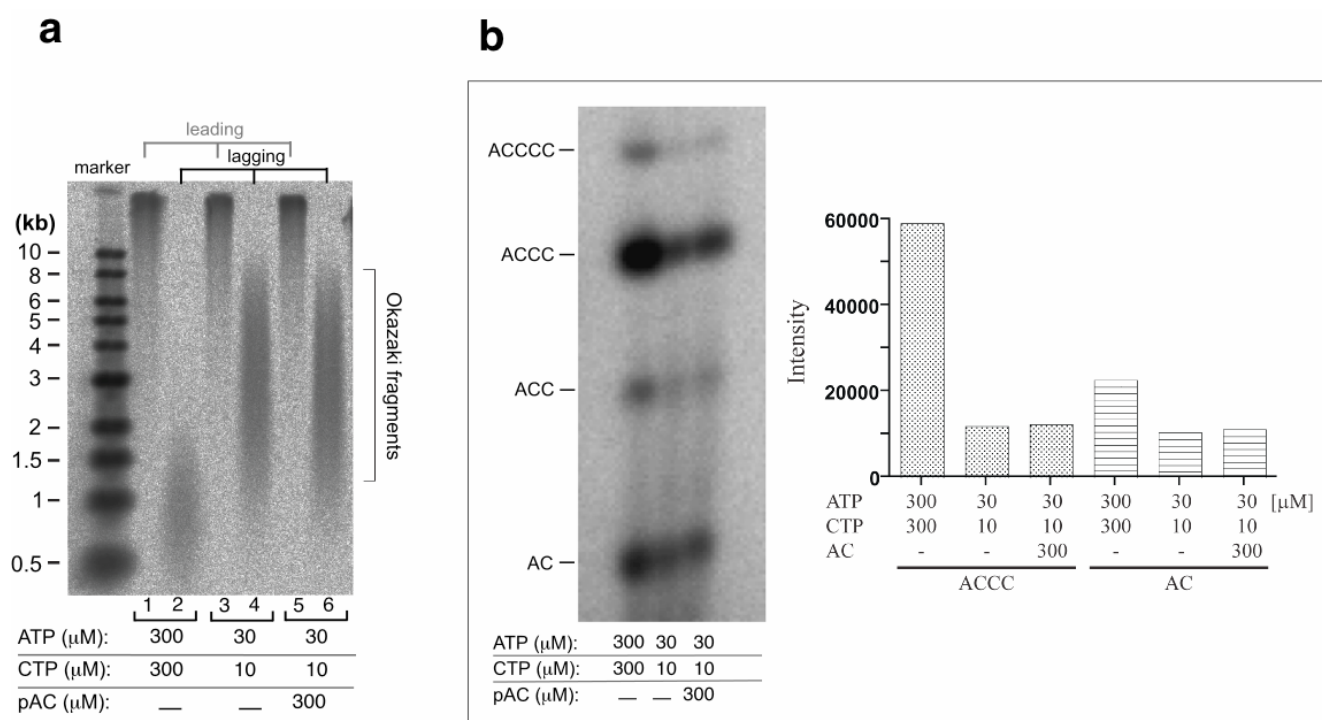


**Figure S6.** (a) In this experiment we performed a bulk-phase characterization of Okazaki-fragment lengths under the same experimental condition used in the single-molecule experiments described in the main text. Coordinated DNA replication reactions were carried out on a rolling mini-circle substrate as described previously<sup>11</sup> with slight in the substrate to allow us to differentiate synthesis at the leading strand from that on the lagging strand using [ $\alpha$ -<sup>32</sup>P]dTMP and [ $\alpha$ -<sup>32</sup>P]dAMP, respectively. The sequences used in constructing the mini-circle are: 5'-CCA CCC CAA AAA CAC CAA CAA CCC AAC ACC ACA CAA CAC ACC ACA AAA CCA CAC GAC CAA AAC CAC CAC C-3' for the 70-base circle and 5'-TTT TTT TTT TTT TTT TTT TTT TTT TTT TTT TTT TTT TTT TTT T T GGT GGT GGT TTT GGT CGT GTG GTT TTG TGG TGT GTT GTG TGG TGT TGG GTT GTT GGT GTT TTT GGG GTG G-3' for the complementary strand to the mini-circle which will result in a 5' overhang. Preparation of the mini-circle is identical to that described previously<sup>11</sup>. The replication reaction is carried out for 5 min at 30 °C, under reaction conditions identical to those used in the single-molecule experiment with a mini-circle concentration of 20 nM. The rolling-circle substrate is designed in a way that leading-strand synthesis is monitored by incorporation [ $\alpha$ -<sup>32</sup>P]dTMP and lagging-strand synthesis by [ $\alpha$ -<sup>32</sup>P]dAMP. Products were visualized on 0.8% alkaline agarose gel. The intensity profile of Okazaki fragments from the gel was rescaled to obtain length distributions from which mean Okazaki fragment lengths were obtained. The presence of both high-molecular weight leading-strand products (lane 1) and lagging-strand products of much shorter length (lane 2) is visible. The length of the low-molecular weight Okazaki fragments (0.8 kb) corresponds well with half of the mean loop length from the single-molecule experiments (1.4 kb/2 = 0.7 kb). Lowering ATP and CTP concentrations increases the Okazaki fragment length by 2-fold (lane 4) in agreement with the 2-fold increase in loop length (Fig. 3, main text). However, pAC could not restore the Okazaki fragment length (lane 6) as it did for the loop length (Fig. 3, main text).

(b) Effect of lowering ATP and CTP concentrations on the kinetics of primer synthesis (experimental conditions as described in (a)). Primer synthesis by gene 4 is measured by its ability to incorporate radioactively labeled CTP into oligoribonucleotides using synthetic DNA template containing the primase recognition sequence 5'-GGGTC-3' as described previously<sup>12</sup>. The reaction (10  $\mu\text{l}$ ) contains gene 4 (1  $\mu\text{M}$ ), the template 5'-GGGTCAA-3' (10  $\mu\text{M}$ ), 0.1 mM each ATP and CTP, 0.1  $\mu\text{Ci}$  of [ $\alpha$ -<sup>32</sup>P]CTP, 40 mM Tris-HCL, pH 7.5, 10 mM MgCl<sub>2</sub>, 10 mM DTT, and 50 mM potassium glutamate. The reaction was incubated for 30 min at 37 °C. The reaction was stopped by adding  $\mu\text{l}$  of sequencing dye (98%

formamide, 10 mM EDTA, pH 8.0, 0.1% xylene cyanol FF, and 0.1% bromo-phenyl blue) and loaded onto 25% denaturing polyacrylamide sequencing gel containing 3 M urea. The radioactive incorporation was analyzed using Fuji BAS 1000 Bioimaging analyzer and the bands were quantified by Image Gauge (Fuji Photo Film, Tokyo). The data show that upon lowering ATP and CTP concentrations, the two steps of primer synthesis are each differently affected. Formation of pppAC decreased by 2 fold while the extension step decreased by 5 fold. Upon providing the reaction with pAC, we did not observe changes in the kinetics of primer synthesis. Upon decreasing ATP and CTP concentrations, the extension step is significantly more affected than the condensation step. These results validate the experimental approach described in the main text as a means to differentiate between the relative contributions of pAC formation and extension to loop release. Furthermore, the data shown here suggest that a failure of primer extension at low ATP/CTP concentrations causes the Okazaki fragment length to remain unaffected by the preformed pAC. The ability of the preformed pAC to restore the replication loop length but not the Okazaki fragment length suggests that replication loop release can take place before the nascent Okazaki fragment is finished.

### Lag time between subsequent loops released by signaling and by collision

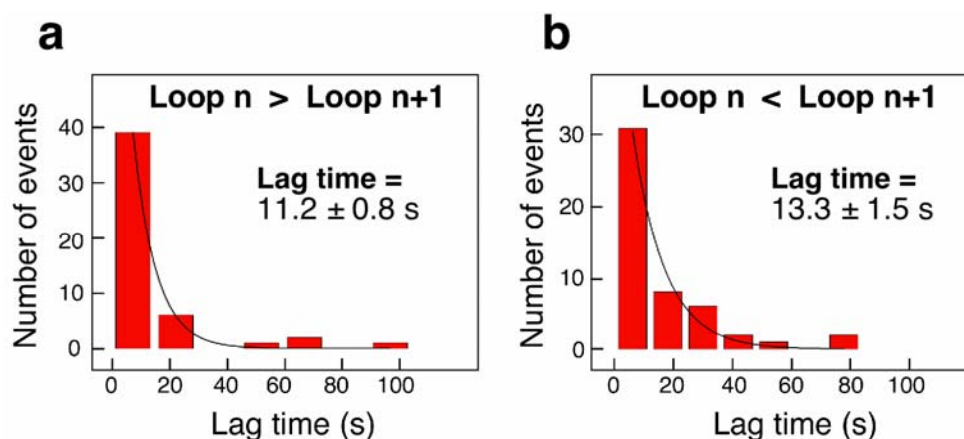


**Figure S7.** The lag time between release of a loop and formation of the next one for pairs in which the first loop release is longer than the second one (Panel 9a); loop  $n > \text{loop } n+1$ , and those in which the first loop is shorter than the second one (Panel (b); loop  $n < \text{loop } n+1$ ).

### Shifting the balance towards the signaling mechanism



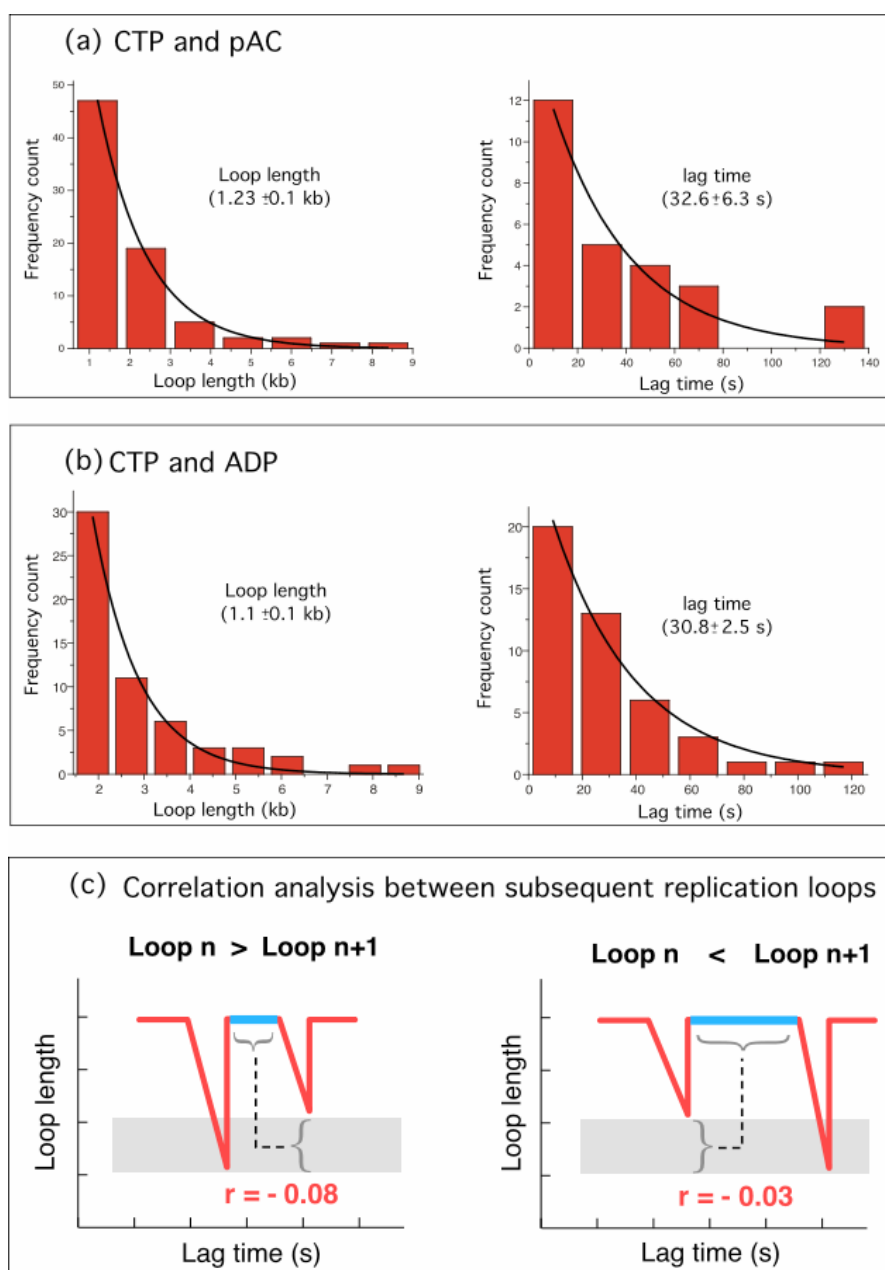


**Figure S8.** We can force the replisome to preferentially use the signaling mechanism as a trigger for loop release by decreasing the rate with which full-length primers are made, but maintaining the rate at which pAC is formed. In these experiments, we maintained the kinetics of the pAC formation step but forced the failure of the extension step by limiting primer synthesis to only one of the four primase recognition sequences. (a) In one experiment, we accomplished this by providing the reaction with pAC (300  $\mu$ M) with only CTP (300  $\mu$ M); a condition that limits primer extension to only those recognition sequences that support the synthesis of a pACCC primer. (b) In another experiment we replaced ATP with ADP (300  $\mu$ M) while keeping CTP (300  $\mu$ M) in the reaction. ADP can be condensed with CTP efficiently to form ppAC but it cannot be extended, limiting the primer extension step to a ppACCC primer. In both experiments the loop length remained unchanged, but the lag time increased by 3-fold. The unchanged loop length in these two experiments further confirms that pAC controls loop release. The increase in length of lag time supports the notion that the formation of full-length primers is frequently aborted. After all, only one of four sequences support the formation of a full-length primer while all four sequences support formation of (p)pAC. As a result, additional leading-strand synthesis must take place during the lag time to encounter a priming site that can be fully utilized. (c) We determined the

*correlation coefficients between the difference in length of pairs of replication loops and the lag time from the experiments described in (a) and (b) (similar to the analysis described in the main text in figure 4). Interestingly, we did not observe any correlation between the lag time and the difference in length of subsequent replication loops in both loop-pair categories. This observation confirms that inefficient primer utilization and a subsequent increase in single-stranded DNA template size may result in an increase in Okazaki fragment size, but that loop release will still be triggered by the stochastic condensation of ATP and CTP and will remain uncorrelated with lag time.*

## REFERENCES

1. Lee, J. B. et al. DNA primase acts as a molecular brake in DNA replication. *Nature* **439**, 621-624 (2006).
2. Bustamante, C., Marko, J. F., Siggia, E. D. & Smith, S. Entropic Elasticity of  $\lambda$  Phage DNA. *Science* **265**, 1599 (1994).
3. Dessinges, M. N. et al. Stretching single stranded DNA, a model polyelectrolyte. *Physical Review Letters* **89** (2002).
4. Mills, J. B., Vacano, E. & Hagerman, P. J. Flexibility of single-stranded DNA: Use of gapped duplex helices to determine the persistence lengths of poly(dT) and poly(dA). *Journal of Molecular Biology* **285**, 245-257 (1999).
5. Park, K., Debyser, Z., Tabor, S., Richardson, C. C. & Griffith, J. D. Formation of a DNA loop at the replication fork generated by bacteriophage T7 replication proteins. *Journal of Biological Chemistry* **273**, 5260-5270 (1998).
6. Nossal, N. G., Makhov, A. M., Chastain, P. D., Jones, C. E. & Griffith, J. D. Architecture of the bacteriophage T4 replication complex revealed with nanoscale biopointers. *Journal of Biological Chemistry* **282**, 1098-1108 (2007).
7. Tabor, S. & Richardson, C. C. A Single residue in DNA polymerases of the *Escherichia coli* DNA polymerase I family is critical for distinguishing between deoxy- and dideoxyribonucleotides. *Proceedings of the National Academy of Sciences of the United States of America* **92**, 6339-6343 (1995).
8. Kolodner, R. & Richardson, C. C. Replication of duplex DNA by bacteriophage T7 DNA-polymerase and gene 4 protein is accompanied by hydrolysis of nucleoside 5'-triphosphates. *Proceedings of the National Academy of Sciences of the United States of America* **74**, 1525-1529 (1977).
9. Lee, J., Chastain, P. D., Griffith, J. D. & Richardson, C. C. Lagging strand synthesis in coordinated DNA synthesis by bacteriophage T7 replication proteins. *Journal of Molecular Biology* **316**, 19-34 (2002).
10. Chastain, P. D., Makhov, A. M., Nossal, N. G. & Griffith, J. Architecture of the replication complex and DNA loops at the fork generated by the bacteriophage T4 proteins. *Journal of Biological Chemistry* **278**, 21276-21285 (2003).
11. Lee, J., Chastain, P. D., Kusakabe, T., Griffith, J. D. & Richardson, C. C. Coordinated leading and lagging strand DNA synthesis on a minicircular template. *Molecular Cell* **1**, 1001-1010 (1998).
12. Lee, S. J. & Richardson, C. C. Essential lysine residues in the RNA polymerase domain of the gene 4 primase-helicase of bacteriophage T7. *Journal of Biological Chemistry* **276**, 49419-49426 (2001).